

## Enhanced Photocatalysis of Methylene Blue by GO/SnO<sub>2</sub> Nanocomposites: A Public Health Perspective

Williams Uyo Queen<sup>1</sup>, Tensaba Andes Akafa<sup>2\*</sup>, Ayara Charles<sup>3</sup>, Eric Agim Agaba<sup>4</sup>, Williams Oche Ujah<sup>5</sup>

<sup>1</sup>Faculty of Science and Technology, Department of Chemical Sciences, Bingham University Abuja-Keffi Rd, New Karu 961105, Nasarawa, Nigeria

<sup>2</sup>Department of Community and Family Medicine, Faculty of Clinical Sciences, Federal University, Wukari, Taraba State, Nigeria

<sup>3</sup>Faculty of Basic Medical Sciences, Department of Human Anatomy, Bingham University, Abuja-Keffi Rd, New Karu 961105, Nasarawa, Nigeria

<sup>4</sup>Faculty of Basic Medical Sciences, Department of Anatomical Sciences, University of Calabar, Calabar, Cross River State, Nigeria

<sup>5</sup>Faculty of Basic Medical Sciences, Department of Anatomy, Bingham University, Abuja-Keffi Rd, New Karu 961105, Nasarawa, Nigeria

DOI: <https://doi.org/10.36348/sjmps.2025.v11i03.011>

| Received: 17.02.2025 | Accepted: 25.03.2025 | Published: 27.03.2025

\*Corresponding author: Tensaba Andes Akafa

Department of Community and Family Medicine, Faculty of Clinical Sciences, Federal University, Wukari, Taraba State, Nigeria

### Abstract

This study successfully synthesized SnO<sub>2</sub> nanoparticles via co-precipitation and subsequently loaded them with varying weight percentages (1-4%) of graphene oxide (GO) using a hydrothermal method. The resulting GO/SnO<sub>2</sub> nanocomposites were comprehensively characterized using a suite of spectroscopic techniques, including SEM, TEM, XRD, elemental mapping, EDX, FT-IR, BET, PL, UV-Vis, and DRS. These analyses confirmed the successful formation of the desired nanostructures. Furthermore, the photocatalytic performance of the nanocomposites and pure SnO<sub>2</sub> was evaluated by monitoring the photodegradation of methylene blue under visible light irradiation, demonstrating the impact of GO loading on photocatalytic activity. The degradation efficiencies of the GO/SnO<sub>2</sub> were much higher than that of pure SnO<sub>2</sub>. From the results obtained, we believe that this current study will provide relevant views for further fabrication of other novel nanostructures and exploration of their potential carcinogenic and environmental consequences.

**Keywords:** Nanocomposites, Photocatalysis, Graphene Oxide, Methylene Blue, Characterization.

**Copyright © 2025 The Author(s):** This is an open-access article distributed under the terms of the Creative Commons Attribution 4.0 International License (CC BY-NC 4.0) which permits unrestricted use, distribution, and reproduction in any medium for non-commercial use provided the original author and source are credited.

## INTRODUCTION

The usage of dyes as coloring agents in textile, paper, cosmetics, pharmaceutical, leather and food industries has attracted much attention over the years (Elshypany, 2021 & Helmy *et al.*, 2018). This can be as a result of certain effects such as the contamination of water which mostly results from the textile industry discharge and the consequences of these is attributed to the fact that dye molecules are difficult to remove, majority of these colored dyes are of synthetic origin and usually consist of aromatic rings in their molecular structure, Inert and non-biodegradable when discharged into waste water without proper treatment (Sanakousar *et al.*, 2022 & Giahi *et al.*, 2019). Therefore, removal of such dyes from waste water requires urgency in a bid to protect human health and environmental resources. Methylene blue (MB), one of the most commonly used base dye, is considered to have multiple uses in the

printing and dyeing industry (Elaouni *et al.*, 2022). In spite of the importance of MB in many industries, its presence in the environment can be bridged if not managed effectively (Jiang *et al.*, 2021). MB is carcinogenic and does not degrade easily due to the characteristic stability of the aromatic rings in its molecular structure (Sanakousar *et al.*, 2022). Traditional biological, chemical and physical techniques such as adsorption and chemical precipitation are recognized for the treatment of waste water from dyeing industries in order to avert any public health crisis among biological beings (Kayode *et al.*, 2015). These methods are expensive, form sludge or generate secondary pollutants, such as dye adsorption on activated carbon, where the pollutant is only converted from the liquid phase to the solid phase, causing pollution. Therefore, the decomposition of dyes into non-toxic compounds is essential and recommended (Lei, & Liu, 2022). The Advanced oxidation processes (AOP) are presently

attracting a great deal of consideration in the field of water treatment (Gusain *et al.*, 2019). These processes involve the use of mixture of photocatalysts composed of semiconductor heterojunctions (Mubarak *et al.*, 2022). Photocatalyst semiconductors such as tin dioxide (SnO<sub>2</sub>) has attracted research interest recently, this is due to its high chemical stability, anti-photo-corrosion, powerful oxidation strength, non-toxicity, low cost, and outstanding catalytic performance (Aniket *et al.*, 2016).

However, the application of SnO<sub>2</sub> for the photodegradation of organic pollutants in aqueous matrices suffers from quick recombination of photogenerated electron-hole pairs, small surface area and the low solar energy conversion efficiency (Binaya *et al.*, 2021) owing to its large band gap of 3.6 eV. Hence, SnO<sub>2</sub> absorbs only UV light but visible light inactive (Aniket *et al.*, 2016). This study, therefore focuses on fabricating a novel photocatalyst that is capable of harnessing these limitations by modifying the structure of SnO<sub>2</sub> through doping with graphene oxide (GO) (Binaya *et al.*, 2021 and Kent *et al.*, 2011) as well as the photocatalytic behaviors of the photocatalysts. The doping of semiconductors with Graphene Oxide (GO) is considered to be an attractive method as GO has the ability to drive charge separation efficiently, extend the lifetime of the charge carriers, and enhance the efficiency of the interfacial charge transfer to adsorbed dyes (Heba *et al.*, 2023) due to its exceptional electrical conductivity and extremely efficient adsorption. Graphene oxide is a two-dimensional material with sp<sup>2</sup> bonded carbon atoms arranged in a honeycomb lattice known for its supportive nature in photocatalytic application due to its extraordinary advantages, such as large theoretical specific surface area (2630m<sup>2</sup>/g) superior electronic and excellent chemical stability (Dong *et al.*, 2012).

### Reagents and Materials

Graphene oxide, Stannous Chloride di-hydrate (98%), ammonia solution (25%), hydrochloric acid (37%), ethanol, methanol, and methylene blue (MB) were all purchased from Sigma Aldrich South Africa. Deionized water was used throughout this experiment. All chemicals used for this study were of analytical grade and used as received.

### Preparation of Tin-Oxide (SnO<sub>2</sub>)

SnO<sub>2</sub> was prepared using the liquid phase co-precipitation method. About 2g of Stannous Chloride di-hydrate (SnCl<sub>2</sub>·2H<sub>2</sub>O) was dissolved in 100ml deionized Water in a beaker after which ammonia solution (25%) was added drop wise with constant stirring. The resulting gel-type precipitate form was filtered off and dried at 80°C for 24 hours to remove water molecules. Finally, tin oxide nano-products was obtained through calcination at 550°C for 4-6 hours.

### Preparation of Graphene Oxide-Tin Oxide (GO-SnO<sub>2</sub>) Nanocomposite

About 1g of SnO<sub>2</sub> nanosheet was dispersed in 120ml beaker and ultrasonicated for 45min at room temperature. The sonicated SnO<sub>2</sub> suspension was stirred continuously at room temperature for 45min followed by the addition of different masses of GO (10,20,30,50 mg) to different aliquots to achieve equivalent weight percentages of 1,2,3 & 4 respectively. The resulting homogeneous mixtures was stirred, afterwards, 3ml of HCl was added to each of them. The resulting suspensions was stirred again for another 45min and then transferred into a 100ml Teflon-lined stainless autoclaves and kept at 180°C in an oven and allowed to cool to room temperature. The resulting precipitates of the different coupled amounts of GO nanocomposites was obtained via centrifugation and thereafter, washed severally with deionized water and ethanol. It was dried overnight in a hot air oven at 80°C to obtain needle like GO-SnO<sub>2</sub> nanocomposites which was grinded into GO-SnO<sub>2</sub> nano-powder.

### Evaluation of the Photocatalytic Activity

The photocatalytic ability of the photocatalysts were measured by the degradation rate of methylene blue (MB) under visible light. 50mg of the synthesized SnO<sub>2</sub> as well as the various weight percentages of GO/SnO<sub>2</sub> (1%, 2%, 3% & 4%) was generally dissolved in 100ml of MB aqueous solution (10mg/L) at room temperature. Before irradiation, the solution was stirred well under dark conditions for 30min to attain adsorption/desorption equilibrium. 5mL of solution was taken every 20min for analysis under a UV-visible spectrometer for 180min. The visible light used in this test was replaced by a xenon lamp of 10W capacity. The degradation efficiency of MB was determined using the equation given below:

$$\text{Photodegradation efficiency (\%)} = [(C_0 - C_t) / C_0] \times 100\% \dots\dots\dots (1)$$

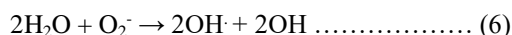
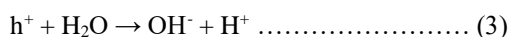
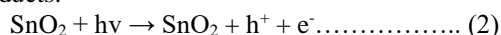
Where C<sub>0</sub> is the initial concentration of MB, C<sub>t</sub> is the concentration of MB at time, t.

### Mechanisms of SnO<sub>2</sub> Photocatalysts for the Degradation of MB

The mechanism of the photocatalytic reaction in the presence of SnO<sub>2</sub> photocatalysts comprises of a free radical reaction initiated by light irradiation (Loh *et al.*, 2010) When the energy of solar radiation exceeds the bandgap of SnO<sub>2</sub> (i.e., photon energy reaches or exceeds its bandgap energy), the surface of the photocatalyst becomes excited, and the electrons transit from the valence band (VB) to the conduction band (CB). In the CB, corresponding electron holes are derived in the VB at the same time, forming electron-hole pairs (i.e., generating electron (e) and hole (H<sup>+</sup>) pairs). VB holes have strong oxidation reaction activity (1.0~3.5 V) because they lose electrons and act as reducing agents, and electrons in the conduction band have good reducibility 0.5~1.5 V when they undergo reduction. Under light irradiation, positive holes and electrons are

generated in the VB ( $h\nu^{+vb}$ ) and CB ( $e^{-}cb$ ) of  $SnO_2$ . These holes can either form hydroxyl radicals or react directly with organic molecules which subsequently oxidize the organic molecules. The electrons can also react with organic compounds to produce reduction products. (Lin *et al.*, 2013)

The role of oxygen is important as it reacts with the photogenerated electrons. Organic compounds can then undergo oxidative degradation through their reactions with hydroxyl and peroxide radicals, VB holes, as well as reductive cleavage via reactions with electrons yielding various byproducts and finally mineral end-products.



### Characterization

The X-ray diffraction pattern of the prepared nanocomposites were obtained using a Shimadzu 6100 X-ray diffractometer with a  $CU\ K\alpha$  radiation source (Bruker D6). The UV-Vis diffuse reflectance spectra (DRS) of the synthesized  $SnO_2/GO$  composites were measured with Perkin-Elmer UV-Vis spectrophotometer, the photoluminescence (PL) emissions were obtained via Perkin Elmer LS 55

spectrofluorometer. The BET analysis (Micrometrics Tristar 3000) of the synthesized composites were carried out to determine their specific surface areas and their textural characteristics. Their surface morphologies were also determined using the Scanning Electron Microscopy instrument (Zeiss 10 kV field). Elemental analysis of the composites was also carried out by energy dispersive spectrometry (EDS, Shimadzu), while the interfacial interaction within the synthesized composites were obtained via High-resolution transmission electron microscopy (JEOL TEM), along with the selected area electron diffraction (SAED) pattern. The FTIR of the composites were measured on Perkin Elmer Series 100 Spectrum to determine the functional characteristics of the composites.

## RESULT AND DISCUSSION

### Structural Analysis

Fig 4.1 the principal diffraction peaks are at  $2\theta$  degrees 26.54, 34.02, 38.03, 51.72, 54.50, 65.88, and 78.54 corresponding to (110), (101), (200), (211), (002), (301), and (202) crystal planes which is compatible with the creation of pure cassiterite  $SnO_2$  crystallite free of impurities. The results illustrated above suggests that there is a gradual increase in peak intensities corresponding to the loading of varying quantities of graphene oxide (GO). Furthermore, the characteristic peaks of GO are absent from the GO- $SnO_2$  composites due to the modest proportion of GO in these materials. Ultimately, the lack of additional peaks in the nanocomposite demonstrated that the photocatalysts were completely free of contaminants in their prepared state.

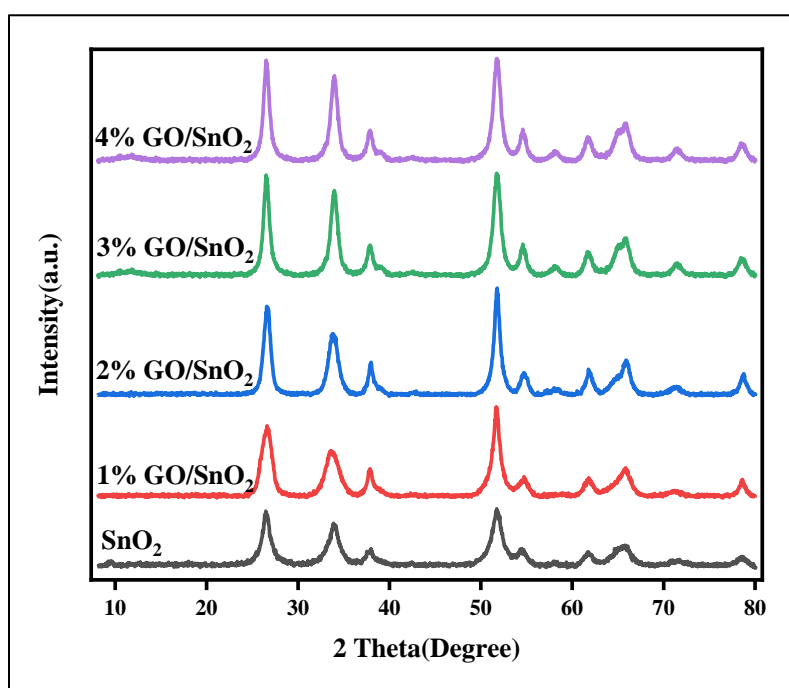


Figure 4.1: XRD patterns of  $SnO_2$  and its respective GO- $SnO_2$  composites

Fig 4.2 There are several peaks present in the pure SnO<sub>2</sub> nanoparticles, which correspond to Sn–O and O–Sn–O, respectively, at around 528, and 668 cm<sup>-1</sup>. O–H, CO<sub>2</sub>, and C–O functionality can be attributed to the

peaks at 3448, 1835, and 1724 cm<sup>-1</sup>, respectively. Meanwhile, other functional groups with only slight differences are visible when different weight percentages of GO are incorporated into SnO<sub>2</sub>.

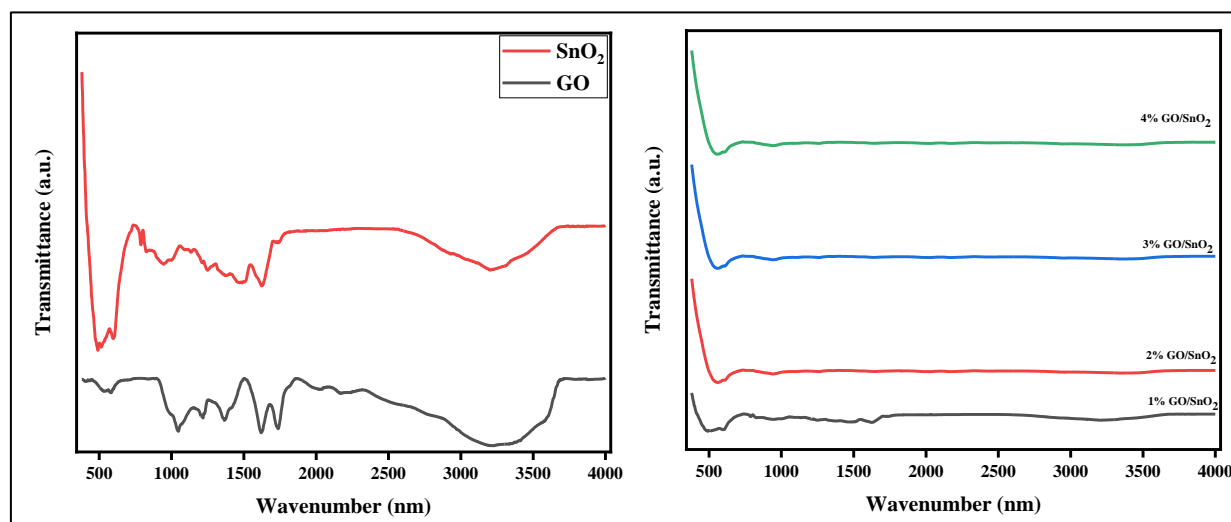


Figure 4.2: FTIR spectra of the synthesized composites

Fig 4.3 The chemical composition of the nanoparticles is confirmed by the EDS of the produced GO-SnO<sub>2</sub> samples, which is also reported. The EDS spectra of the modified GO/SnO<sub>2</sub> showed the presence

of the following element Sn, C, N and O, with C and N having lower atomic percentages which could be as a result of the low weight percentages of GO used in the synthesis.

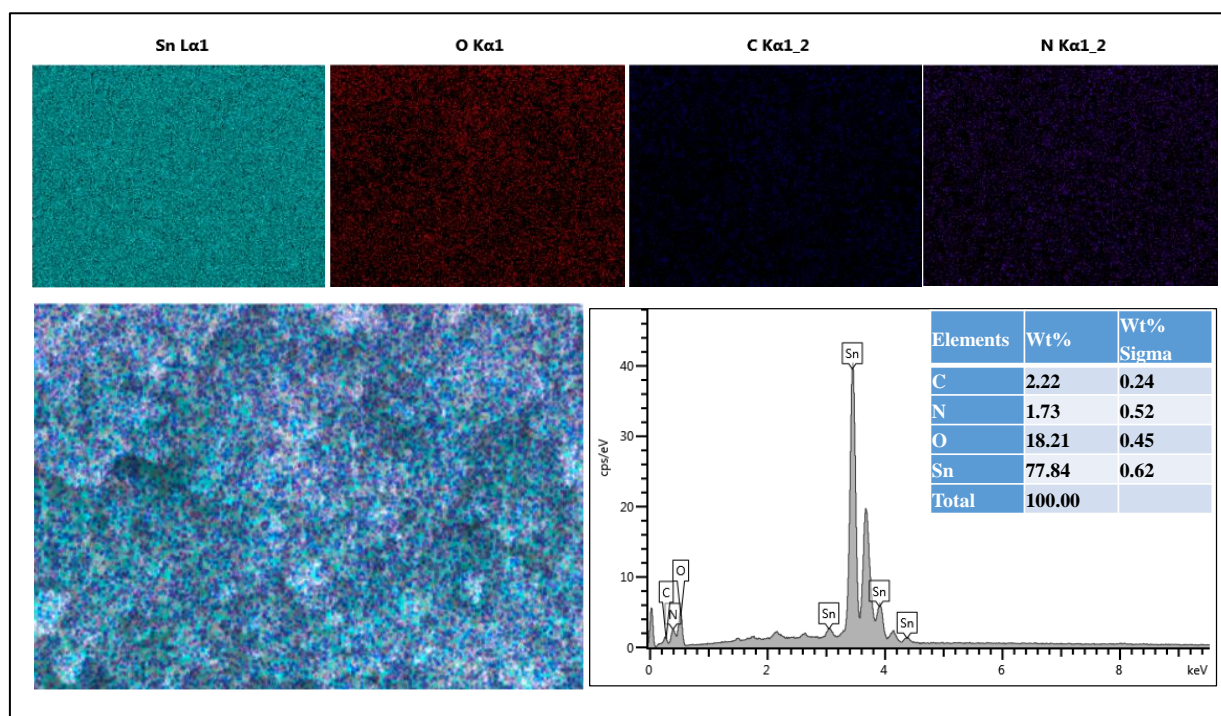


Figure 4.3: SEM-EDS elemental mapping and EDS spectrum of GO-SnO<sub>2</sub>

Fig 4.4 the PL spectrum shows that the SnO<sub>2</sub> peak intensity is decreased by the GO nanosheet when GO serves as an electron sink. It can be seen that the PL spectral intensity of the different masses of the composites of GO/SnO<sub>2</sub> nanocomposites are all lower than that of pure SnO<sub>2</sub> nanoparticle, indicating that there

is a formation junction between GO and SnO<sub>2</sub> which can facilitate photo-generated charge transfer. In addition, 3%GO/SnO<sub>2</sub> shows extremely low PL spectrum intensity, suggesting a noticeable improvement in the suppression of charge recombination (Khan *et al.*, 2013).



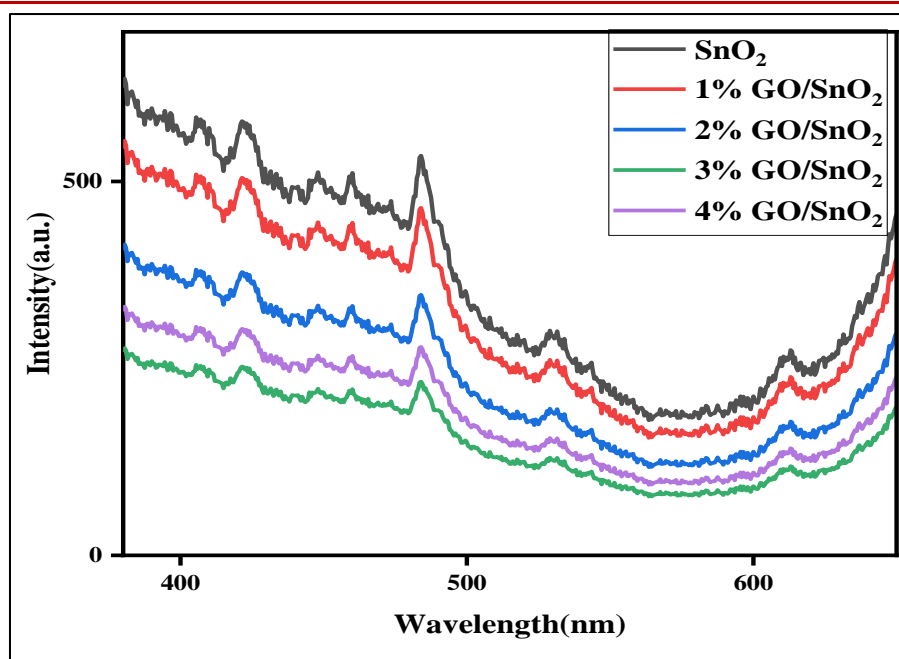


Figure 4.4: PL spectrum of SnO<sub>2</sub> and GO/SnO<sub>2</sub> composites

### Morphological Analysis

Fig 4.5, is evident that graphene oxide (GO) has a sheet-like structure, which is a sign of a well synthesized material while the SnO<sub>2</sub> particles have a surface morphology that is almost uniform, and they

appear to be in a mixed condition that includes both parted and agglomerated forms. It is clear that tiny GO nanoparticles aggregate to form bigger clusters on the surface of SnO<sub>2</sub>, a characteristic shared by all nanocomposite morphologies.

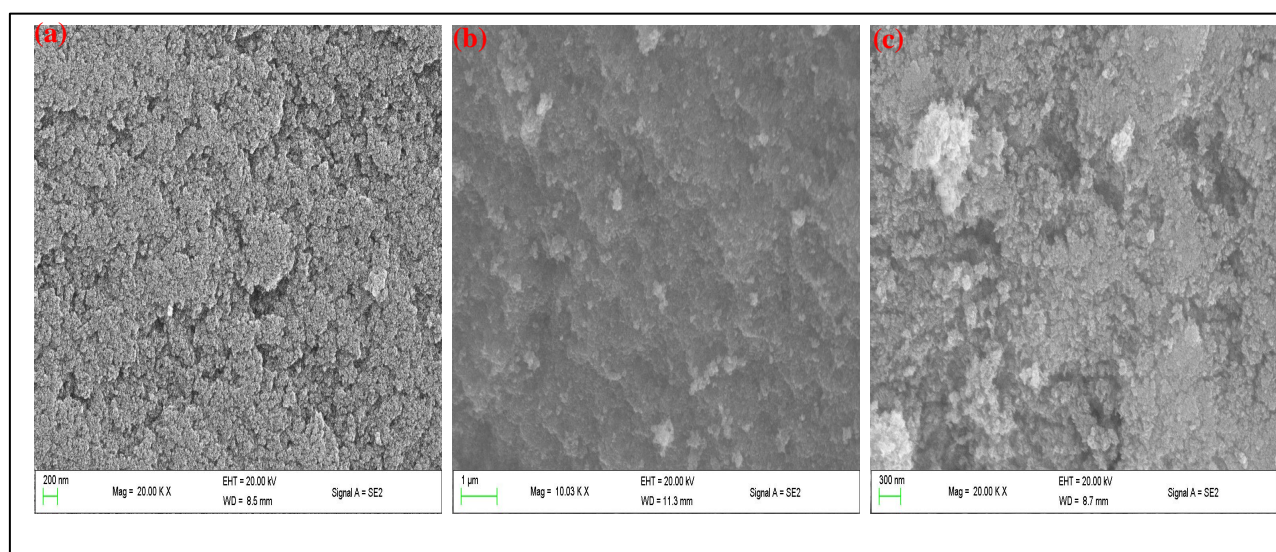
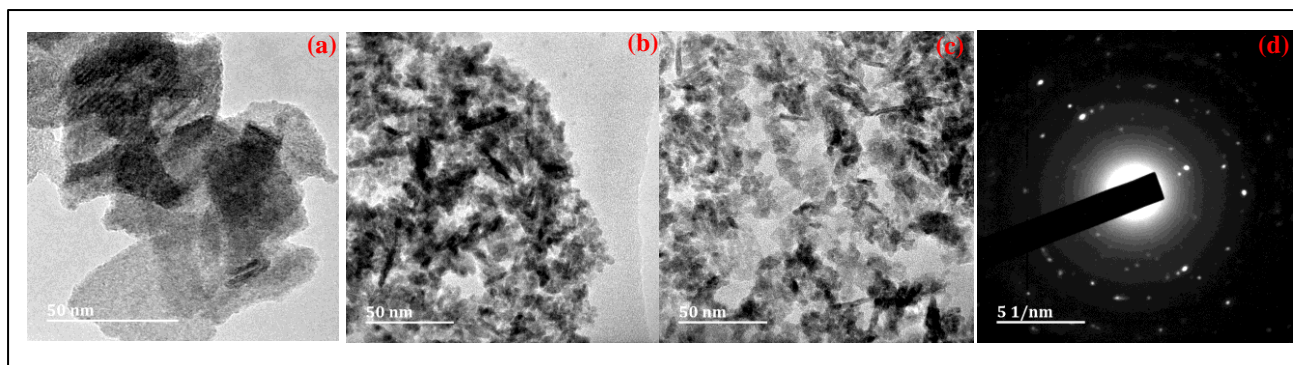


Figure 4.5: SEM image of synthesized (a) GO, (b) SnO<sub>2</sub> and GO/SnO<sub>2</sub> composites

Fig 4.6(b) the TEM pictures reveals that the sheets that make up GO have a curly morphology, with the edges of the sheets somewhat folded and scrolled. The TEM image of SnO<sub>2</sub> nanoparticles depicts an agglomeration of almost tiny spherical particles. As illustrated in Figure 4.5(c), the GO-SnO<sub>2</sub> showed dispersion of GO on the composites of GO-SnO<sub>2</sub> which

means the successful construction of heterojunctions between GO nanosheet and SnO<sub>2</sub> nanoparticles (Lei 2022). The SAED spectrum of the composites in Figure 4.5(d) shows that the crystallinity of the SnO<sub>2</sub> nanoparticle remains intact even with the inclusion of GO purposely due to the low quantity of GO in the composites.



**Figure 4.6:** TEM images of (a) GO, (b) SnO<sub>2</sub>, (c) GO-SnO<sub>2</sub> and (d) SAED spectrum of GO-SnO<sub>2</sub>

Fig 4.7 the GO-SnO<sub>2</sub>, SnO<sub>2</sub>, and synthesized GO surface areas were measured utilizing the nitrogen adsorption and desorption isotherm of a BET analyzer. Adsorption-desorption profile followed type IV characteristic with type H3 hysteresis loop, indicating mesoporous structure development for all the synthesized composites. In comparison to SnO<sub>2</sub>, the synthesized varying masses of the composite materials

showed an increase in BET specific surface area. In particular, the addition of GO, which has a surface area of 1392.28 m<sup>2</sup>/g, caused the surface area of SnO<sub>2</sub> to rise from 12.26 m<sup>2</sup>/g to 39.37 m<sup>2</sup>/g. The cross-sectional area of the pollutants and the adsorption surface area grew together, improving the composite's photocatalytic efficacy.

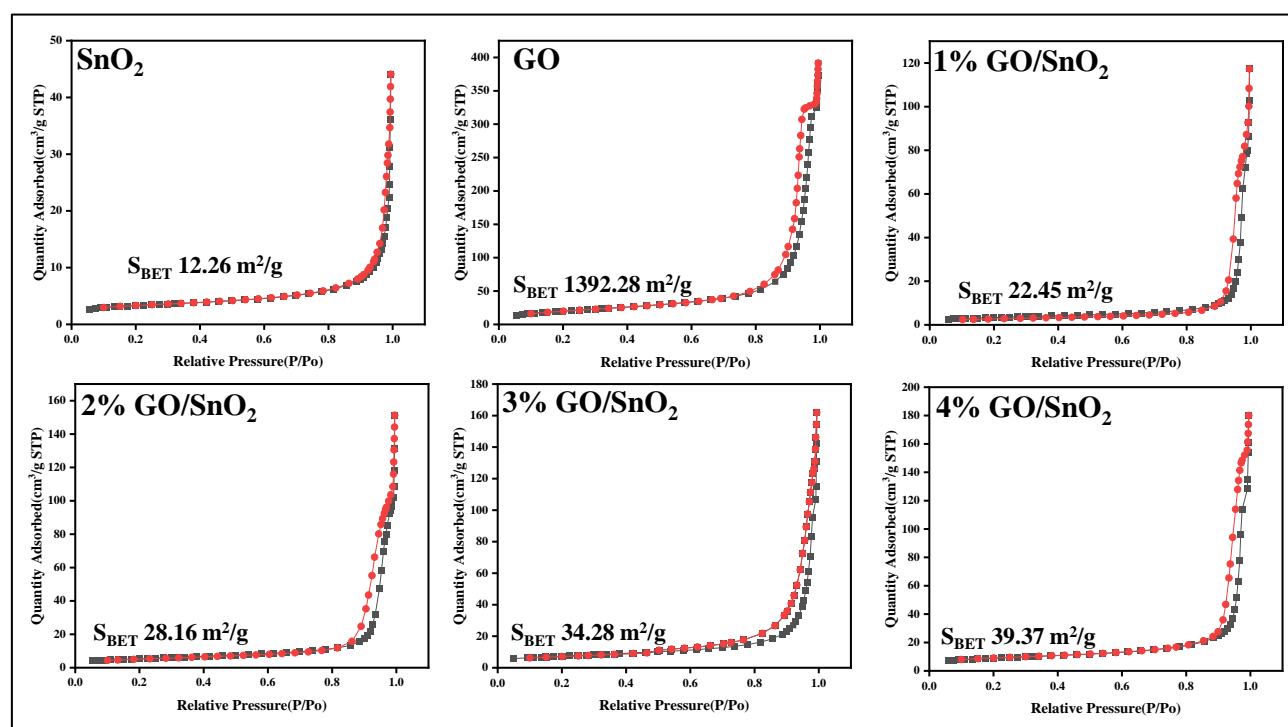


**Figure 4.7:** Nitrogen adsorption-desorption isotherms of the synthesized materials

In fig 4.8a the UV-vis absorption spectra shows that the optical absorption edges of SnO<sub>2</sub> nanoparticles are at about 410 nm, which cannot make full use of visible light while for the difference masses of GO/SnO<sub>2</sub> nanocomposites, the absorption shows a broad elevated background in the visible region with increasing content of GO nanosheet implying that the GO could optimize the optical absorption ability of GO/SnO<sub>2</sub> nanocomposites. This phenomenon indicates that more

solar energy can be absorbed by the photocatalyst, which is beneficial for photocatalytic degradation of organic pollutants. Furthermore, in Figure 8(b), the E<sub>g</sub> (band gap) values of SnO<sub>2</sub> nanoparticles and the difference masses of GO/SnO<sub>2</sub> are 3.12, 2.75 and 2.62 eV, respectively. It is obvious that the optical band gap of GO/SnO<sub>2</sub> nanocomposites is gradually decreased with the increasing amount of GO when compared to pristine SnO<sub>2</sub> nanoparticle.

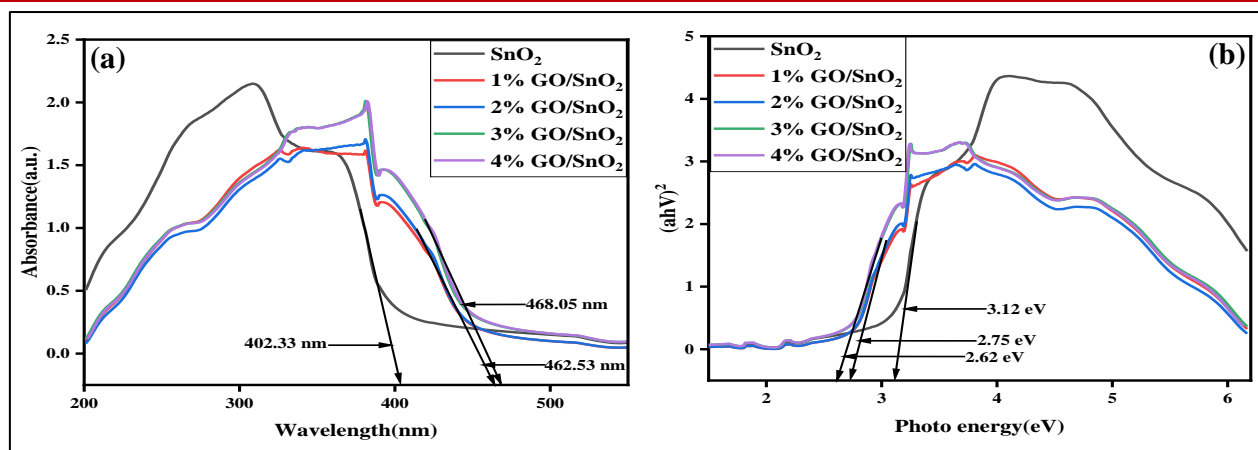


Figure 4.8: (a) UV-vis DRS spectrum and (b) Kubelka-Munk plot of the synthesized composite

### Photocatalytic Performance

Fig 4.9 the photocatalytic performance of SnO<sub>2</sub> and the varied masses (1, 2, 3 & 4) wt. % of GO/SnO<sub>2</sub> nanocomposites achieved degradation efficiencies of 44.70%, 75.18%, 86.97%, 93.42% and 90.01% respectively with methylene blue removal under visible light irradiation in 180 minutes. This indicates that the degradation rate improved with increasing GO content, with optimal performance being reached at 3% GO/SnO<sub>2</sub> weight percentage. Increase in GO content above this weight percentage decreased the amount of photocatalytic activity, probably because the GO aggregated within the SnO<sub>2</sub> nanosheet, reducing its active surface area and introducing recombination sites. Kinetic analyses were employed to compare the methylene blue degradation rate of the composites according to the logarithmic ratio of C<sub>0</sub> (initial concentration of the MB) and C<sub>t</sub> (the concentration of the MB at the time of t), which the following relationship has carried:

$$\ln C_0/C_t = k_{\text{abs}} t$$

Where  $k_{\text{abs}}$  is the rate constant of the absorption. If the  $\ln C_0/C_t$  vs.  $t$  plotting is drawn by matching the data with straight lines, then the slope of these lines will indicate the absorption rate of the samples. These results are presented in Fig. 4.9(b) shows that the 3% GO/SnO<sub>2</sub> nanocomposites show the most excellent  $k(\text{abs})$  which can be attributed to the synergetic effects of GO on SnO<sub>2</sub>.

### Public Health Implications

Graphene-based tin oxide (SnO<sub>2</sub>) composites offer significant potential for photocatalytic applications like methylene blue degradation. However, a prudent evaluation necessitates careful consideration of their potential carcinogenic and environmental consequences. While SnO<sub>2</sub> is generally considered non-carcinogenic, graphene's ability to induce oxidative stress and DNA damage raises concerns (Sanakousar *et al.*, 2022). Furthermore, methylene blue is a known carcinogen, and its degradation may produce harmful byproducts. Environmentally, these composites may contribute to water and soil pollution, with the production process

potentially releasing nanoparticles into the air. Mitigation strategies are crucial. These include safe handling protocols, comprehensive toxicity assessments of both composites and degradation products, the development of green synthesis methods, and the pursuit of biodegradable composite designs. By prioritizing risk assessment and implementing preventative measures, the benefits of graphene-based SnO<sub>2</sub> composites can be realized while minimizing their potential negative impacts on human health and the environment (Sanakousar *et al.*, 2022; Jiang *et al.*, 2021).

### CONCLUSION

The enhanced photocatalytic activity of graphene oxide (GO)-functionalized SnO<sub>2</sub> observed in this study, and its efficacy in removing methylene blue, has a significant implication for the health of the public. While the current conclusion highlights the potential of this composite material for removing carcinogenic organic dyes from water, framing it within a public health perspective amplifies its value. The availability of clean and safe water is a fundamental determinant of public health, and the presence of organic contaminants, including dyes like methylene blue, poses a direct threat through potential carcinogenic effects and other toxicities. This research, therefore, contributes to the development of a cost-effective and easily implemented water remediation strategy. Future studies should focus on scaling up this technology, evaluating its long-term stability, and assessing its effectiveness against a broader spectrum of waterborne contaminants relevant to public health concerns. By emphasizing the link between this photocatalytic approach and the reduction of exposure to harmful substances in drinking water, the scientific value of the research is further enhanced within the context of safeguarding public well-being.

### REFERENCES

- Aniket, K., Lipeeka, R., Satish, K.A., Anurag, M., Rajendra, S.D., Priyabrat, D. (2016). An investigation into solar light driven enhanced photocatalytic properties of a graphene oxide-SnO<sub>2</sub>-TiO<sub>2</sub> ternary nanocomposite. Journal of Royal

- society of chemistry advances. Doi:10.1039/c6ra02067d
- Binaya, K.S., Rabindra, N.J., Madhusmita, S., Ravi, K., Das, A. (2021). Interface of GO with SnO<sub>2</sub> quantum dots as an efficient visible-light photocatalyst. Surface and nanoscience institute. <http://doi.org/10.1016/j.chemosphere.130142>
  - Dong, P., Wang, Y., Guo, L., Liu, B., Xin, S., Zhang, J., Shi, Y., Zeng, W., Yin, S. (2012). A facile one-step solvothermal synthesis of graphene/rod-shaped TiO<sub>2</sub> nanocomposite and its improved photocatalytic activity, *Nanoscale* 4:4641-4649. <https://doi.org/10.1039/c2nr31231j>
  - Elaouni, A. (2022). ZIF-8 metal organic framework materials as a superb platform for the removal and photocatalytic degradation of organic pollutants: A review. *RSC Adv.* 12, 31801–31817.
  - Elshypany, R. (2021) Elaboration of Fe<sub>3</sub>O<sub>4</sub>/ZnO nanocomposite with highly performance photocatalytic activity for degradation methylene blue under visible light irradiation. *Environmental Technology Innovation* 23, 10171
  - Giahhi, M (2019). Preparation of Mg-doped TiO<sub>2</sub> nanoparticles for photocatalytic degradation of some organic pollutants. *Stud. Univ. Babes-Bolyai Chem.* 64, 7–18 .
  - Gusain, R., Gupta, K., Joshi, P. & Khatri, O. P. (2019). Adsorptive removal and photocatalytic degradation of organic pollutants using metal oxides and their composites: A comprehensive review. *Advance College Interface. Science*, 272, 102009.
  - Heba, M.E., Amira, M.S., Rania, E., Hanaa, S. (2023). Efficient photocatalytic degradation of organic pollutants over TiO<sub>2</sub> nanoparticles modified with nitrogen and MoS<sub>2</sub> under visible light irradiation. *Scientific Reports* 13:8845 <https://doi.org/10.1038/s41598-023-35265-7>
  - Helmy, E. T., El Nemr, A., Mousa, M., Arafa, E., Eldafrawy, S. (2018). Photocatalytic degradation of organic dyes pollutants in the industrial textile wastewater by using synthesized TiO<sub>2</sub>, C-doped TiO<sub>2</sub>, S-doped TiO<sub>2</sub> and C, S co-doped TiO<sub>2</sub> nanoparticles. *Journal of Water Environmental Nanotechnology*, 3,116–127.
  - Jiang, D. J., Tunmise, A. O., Yuanyuan, O., Noor, F. S., Song, W., Ailing, Z., Sanxi, L. (2021). A Review on Metal Ions Modified TiO<sub>2</sub> for Photocatalytic Degradation of Organic Pollutants. <https://doi.org/10.3390/catal11091039>
  - Kayode, A.A., Olugbenga, S. B. (2015). Dye sequestration using agricultural wastes as adsorbents, *Water Resource Industry*, 12: 8–24, <https://doi.org/10.1016/j.wri.09.002>.
  - Kent, F.C., Montreuil, K.R., Brookman, R.M., Sanderson, R., Dahn, J.R., Gagnon, G.A. (2011). Photocatalytic oxidation of DBP precursors using UV with suspended and fixed TiO<sub>2</sub>. *Water Resources*: 45: 6173-6180.<https://doi.org/10.1016/j.watres.2011.09.013>
  - Khan, M.M., Ansari, S.A., Amal, M.I., Lee, J., Cho, M.H. (2013). Highly visible light active Ag@TiO<sub>2</sub> nanocomposites synthesized by electrochemically active biofilm: A novel biogenic approach, *Nanoscale*. 5:4427-4435. <https://doi.org/10.1039/c3nr00613a>
  - Lei, C. (2022). Bio-photoelectrochemical degradation, and photocatalysis process by the fabrication of copper oxide/zinc cadmium sulfide heterojunction nanocomposites: Mechanism, microbial community and antifungal analysis. *Chemosphere* 308, 136375.
  - Liu, Z. (2022). High efficiency of Ag<sub>0</sub> decorated Cu<sub>2</sub>MoO<sub>4</sub> nanoparticles for heterogeneous photocatalytic activation, bactericidal system, and detection of glucose from blood sample. *Journal of Photochemical Photobiology B* 236, 112571.
  - Loh, K.P., Bao, Q., Ang, P.K., Yang, J. (2010). The chemistry of graphene, 2277–2289. <https://doi.org/10.1039/b920539j>.
  - Lin, L., Yang, Y., Men, L., Wang, X., He, D., Chai, Y., Zhao, B., Ghoshroyb, S., Tang, Q. (2013). A highly efficient TiO<sub>2</sub>@ZnO n–p–n heterojunction nanorod photocatalyst, *Nanoscale*. 5 588–593. <https://doi.org/10.1039/c2nr33109h>
  - Mubarak, M. F., Selim, H., Elshypany, R. (2022). Hybrid magnetic core–shell TiO<sub>2</sub>@ CoFe<sub>3</sub>O<sub>4</sub> composite towards visible light-driven photodegradation of Methylene blue dye and the heavy metal adsorption: Isotherm and kinetic study. *Journal of Environmental Health Science England* 20, 265–280.
  - Sanakousar, F., Vidyasagar, C., Jiménez-Pérez, V., Prakash, K. (2022). Recent progress on visible-light-driven metal and non-metal doped ZnO nanostructures for photocatalytic degradation of organic pollutants. *Material Science Semiconductor Process*, 140, 106390.